

Supplementary Information

Title:

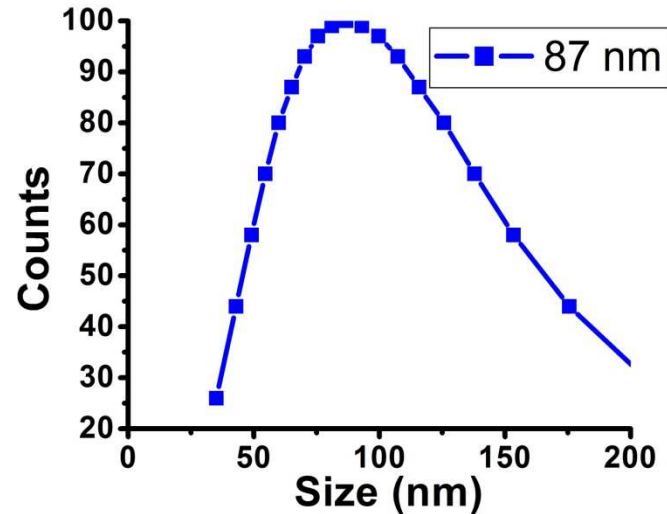
Fluorescent magnetic nanoparticles for magnetically enhanced cancer imaging and targeting in living subjects

Authors:

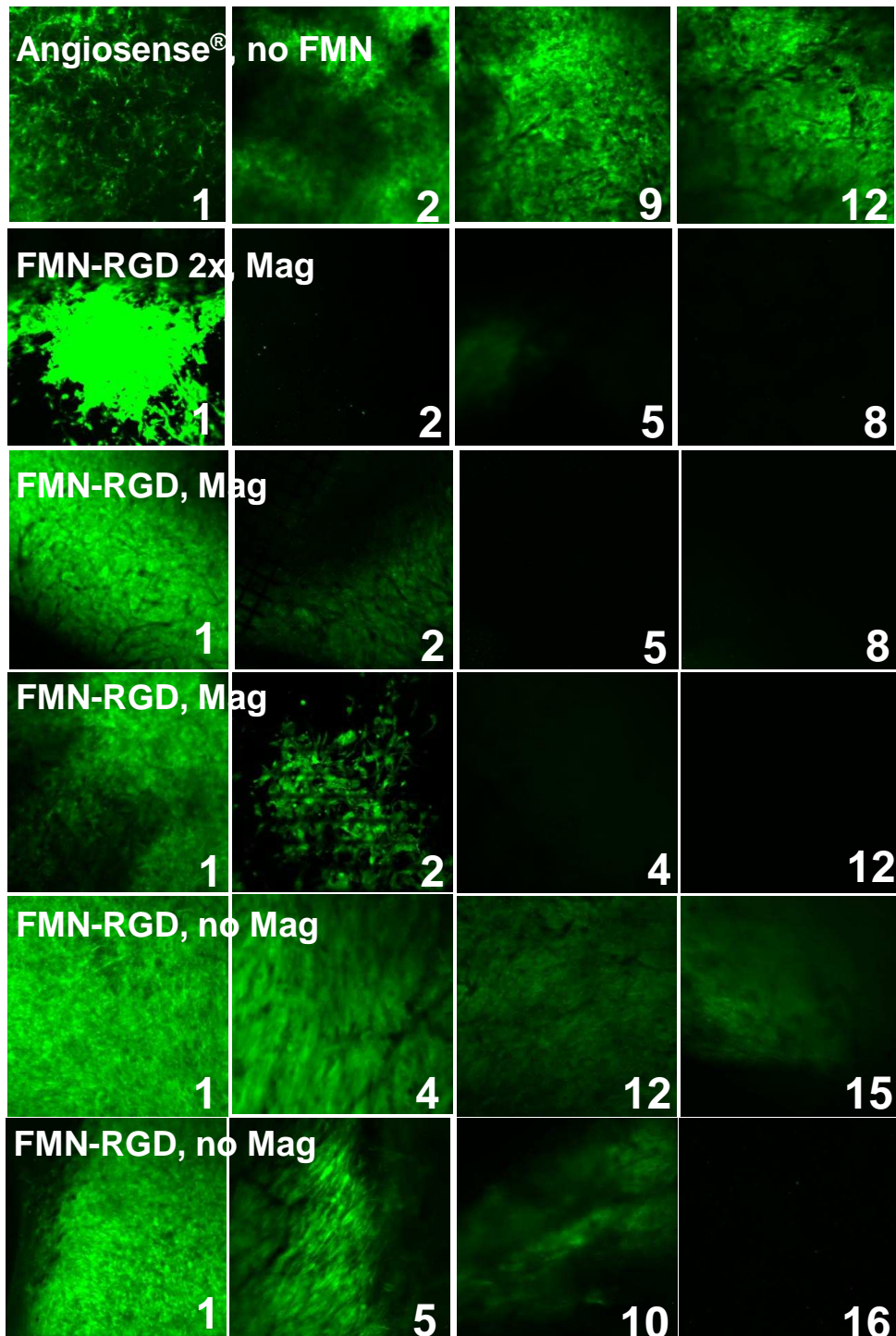
Aihua Fu^{1,3,5*}, Robert Wilson^{1,3}, Bryan Smith^{2,3}, Joyce Mullenix^{1,3}, Chris Earhart^{1,3},
Demir Akin^{2,3}, Samira Guccione², Shan X. Wang^{1,3*}, Sanjiv S. Gambhir^{2,3,4*}

¹Department of Materials Science and Engineering, ²Department of Radiology, ³Molecular Imaging Program at Stanford and ⁴Department of Bioengineering, Bio-X Program, Stanford University, Stanford, California 94305 USA; ⁵NVIGEN Inc, 265 Sobrante Way, suite H, Sunnyvale, Ca 94086.

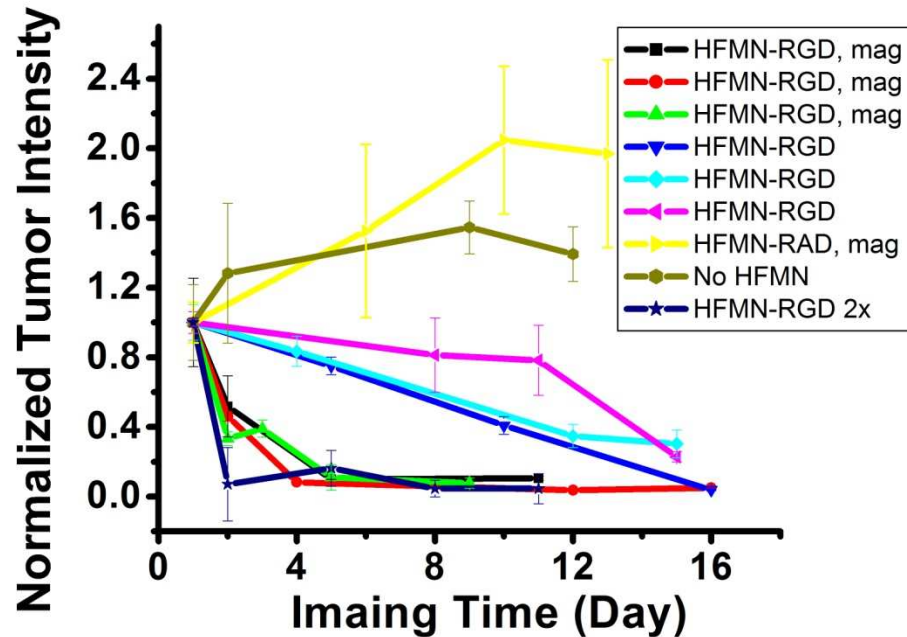
*Correspondence should be addressed to S.S.G. (sgambhir@stanford.edu), S.X.W. (sxwang@stanford.edu), and A. F. (aihuafu@nvigen.com).



Supplementary figure 1. Dynamic light scattering (DLS) measurement showing the size of the SPIO nanoparticles after silanization and prior to fluorophore incorporation. The emission of the Cy5.5 fluorophores prohibited DLS measurement of nanoparticle sizes after fluorophore incorporation, because a red laser is used in the DLS. However, based on DLS measurement of FMN with shorter emission wavelength at 488 nm, the addition of fluorophores added 10 nm to the size of nanoparticles. So, roughly, the estimated size of FMN nanoparticles utilized in this work is 97 nm.

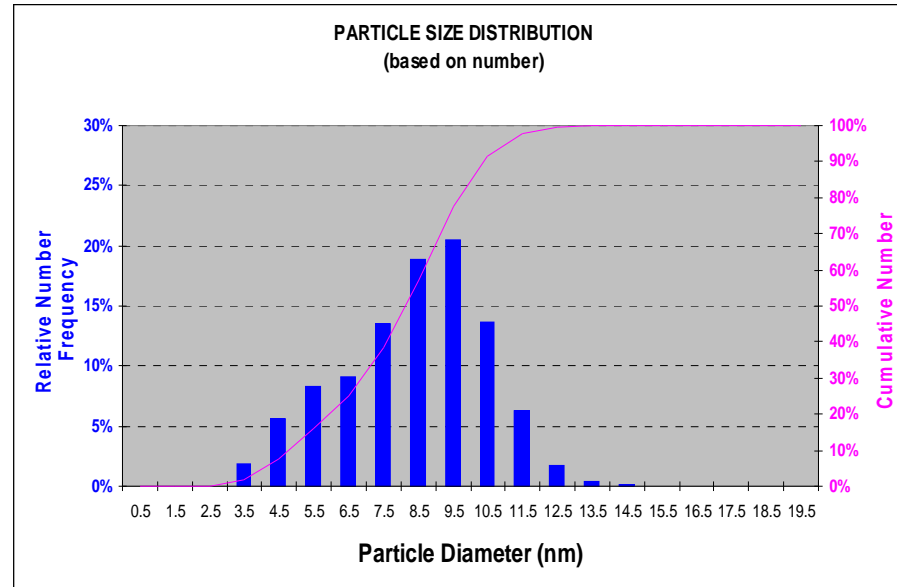
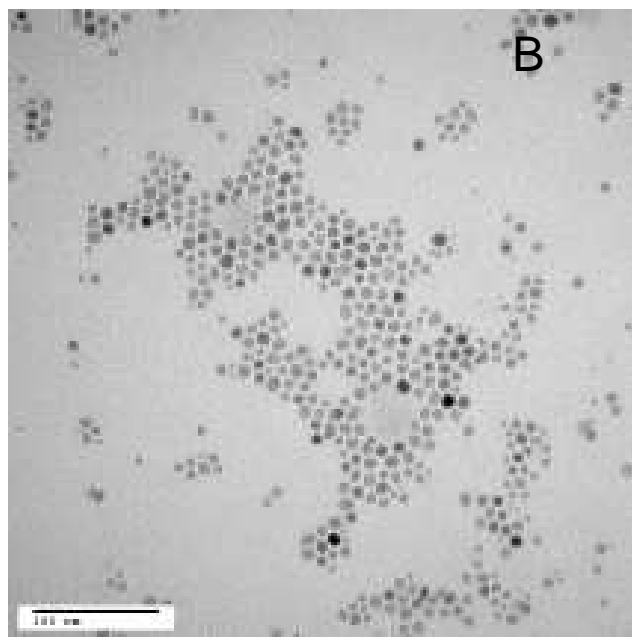


Supplementary figure 2. Tumor intensity change of EGFP transfected U87MG glioblastoma cells following days after FMN injection. The day of sample injection is labeled day 1. A quantitative plot of the tumor intensity change with time is provided in supplementary figure 3. A statistical demonstration of the significant difference between FMN-RGD injection with and without magnetic targeting is provided in Figure 5E. To save space, plots of samples that have already been shown in figure 5A-C are not duplicated here, however, the samples shown in figure 5A-C are included in the quantitative and statistical analysis of supplementary figure 3 and Figure 5E.

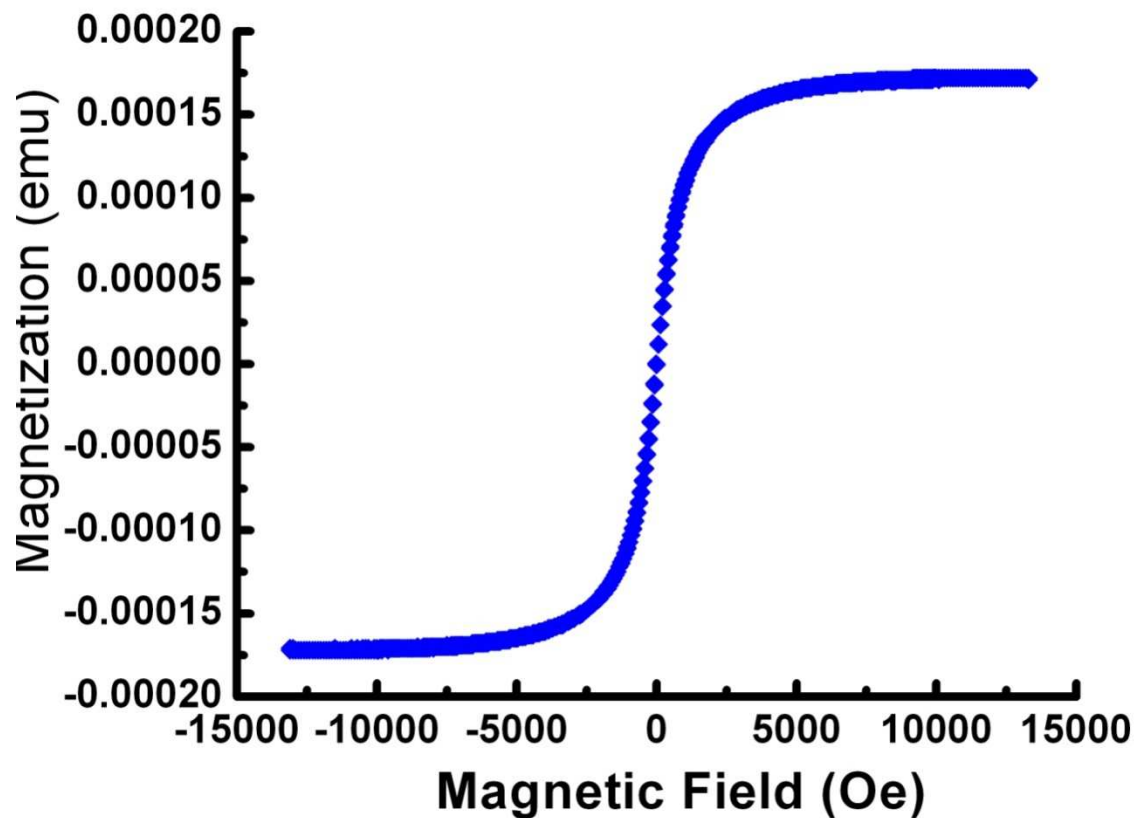


Supplementary figure 3. Quantitative plotting of tumor intensity change with time. Data are based on imaging plots as listed in supplementary figure 2 and Figure 5A-C. The responses of mice to different samples and experimental conditions are manifested. When no FMN-RGD is injected, only injection of Angiosense® did not induce tumor regression (olive curve), same as injection of FMN-RAD (yellow curve). Injection of FMN-RGD at 10 pm dose under magnetic targeting reproducibly (black, red and green) expedited tumor regression compared to 10 pm FMN-RGD injection with no magnetic targeting (blue, turquoise, and pink curves). The deep blue curve shows that increasing the dose of FMN-RGD to roughly 2 fold, but without magnetic targeting, caused the tumor to regress in a similar manner as under magnetic targeting with a dose of 10 pm of FMN-RGD. This indicates that through magnetic targeting, more FMN were retained in the tumor region to expedite tumor regression.

A



Supplementary figure 4. (A) TEM image of SPIO nanoparticles from organic solvent. (B) Size distribution from TEM image analysis (Mean diameter = 8.4 nm, standard deviation = 2.1 nm; particles counted = 3347).



Supplementary figure 5. The magnetization curve of FMN measured using an alternating gradient magnetometer. After determining the Fe mass of the FMN solution measured, using Inductively Coupled Plasma Mass Spectrometry, the saturation magnetic moment of FMN was calculated as 105 emu/g Fe.

Supplementary calculation:

To magnetically retain FMN, the magnetic force exerted on a FMN must be able to overcome the Stokes viscous drag force on the FMN in vessel. Hence the magnetic field gradient required can be calculated from the following equation:

$$3\pi\eta dv = V|\nabla(M \bullet H)|$$

The parameters applied are: Particle diameter $d=100$ nm, Viscosity $\eta=1.5$ centipoise= $1.5 \times 10^{-3} \text{ kg m}^{-1} \text{ s}^{-1}$ ^[1]; Tumor Blood Flow rate $v= 3 \text{ }\mu\text{m/s}$ ^[2]; FMN volume $V=(4/3)\pi(8 \text{ nm}/2)^3$; $\rho=5 \text{ g/cm}^3$; and FMN magnetization (under 2 KOe external field) = 80% x 105 emu/g Fe (supplementary figure 5); $1 \text{ emu}=10^{-3} \text{ A m}^2$; $1 \text{ T}=1 \text{ kg A}^{-1} \text{ S}^{-2}$. After substituting these numbers into the above formula, the calculated magnetic field gradient is estimated at:

$$\nabla H=4 \times 10^4 \text{ T/m}$$

References:

1. Sevick, E. M., Jain, R. K., Viscous resistance to blood flow in solid tumor: Effect of hematocrit on intratumor blood viscosity. *Cancer Research*, 49, 3513-3519, 1989.
2. Hansen-Algenstaedt, N., Joscheck, C., Schaefer, C., Lamszus, K., Wolfram, L., Biermann, T., Algenstaedt, P., Brockmann, M. A., Heintz, C., Fiedler, W., Ruther, W. Long-term observation reveals time-course-dependent characteristics of tumour vascularisation. *European J. Cancer* **41**, 1073-1085 (2005).

Supplementary movie link:

http://www.stanford.edu/group/wang_group/video3/index.html

Supplementary movie captions:

Supplementary movies demonstrate the real time accumulation of FMN through magnetic targeting. These movies begin 4 min after exerting the magnetic force and span 10 min, with each movie containing 60 image frames recorded at 10 s intervals. The movies with red, blue and green signals correspond to the fluorescence from FMN, Angiosense® and EGFP, respectively. The real time accumulation of FMN under the magnetic targeting can be directly observed and the increase in average intensity over the ROI as shown in Fig 3B comes mostly from an increased fluorescent area, rather than increasing peak intensity. In the red FMN signal, If using the small red dot in the upper right position of the ROI (Fig 3A) as a guidance, one will see that when watching the video at time 0, the red dot and the accumulation area are far apart, but at the end of the time movie, the accumulation area grows and joins the red dot. With this guidance, it is more obvious to the eye that accumulation of FMN happened during the time course, and it is clearly reflected in the data analysis with a clear ROI average intensity increase (Fig 3B). The Angiosense® and the tumor EGFP signals show negligible increases in average intensity over ROI with time.